Journal of Engineering Science and Technology
Special Issue on Development of Sustainability Systems - II, 88 - 101

PERFORMANCE ENHANCEMENT OF A SOLAR WATER COLLECTOR USING ALUMINIUM POROUS MEDIUM AND NANOPARTICLES

AHMED H. JASSIM, HASANAIN A. ABDUL WAHHAB*

Training and Workshop Centre, University of Technology, 35050, Baghdad, Iraq
*Corresponding Author: 20085@uotechnology.edu.iq

Abstract

This paper presents an experimental investigation of the solar water collector's performance using an open-cell porous medium with nanoadditives. Experiments were carried out in the solar site of the university of Technology- Iraq. An open cell porous material, made of aluminium with a porosity of 80%, also water and Al_2O_3/water nanofluid at volume concentrations of 2% and 3% as thermal fluids have been used in the experimental solar water heater. The performance evaluation was formed with different flow rates of thermal fluid at 1.5, 2.5, and 3.5 l/min for testing of solar collector performance. The results revealed that the temperature difference between the inlet and outlet decreases with increasing water flow rates through the solar water collector. Also, the results showed that the thermal efficiency of the collector increases with increasing the water flow rate especially at noon. It increased by 5% and 18.4% when using the flow rates 2.5 and 3.5 l/min compared to 1.5 l/min, respectively. Also, the results show that using Al_2O_3/water nanofluid at concentrations of 2% and 3% increases the thermal efficiency by 27.6% and 38.4%, respectively, compared with water alone as a cooling fluid.

Keywords: Nanoadditives, Performance enhancement, Porous medium, Solar energy, Solar water heater.

1. Introduction

Clean energy sources have been harnessed to provide energy in many applications, being a low-cost and environmentally friendly source, as they have diversified to include solar energy, wind energy, geothermal energy, uses of biomass, tidal energy, and other sources [1]. As a result of the availability of safety in use, solar energy became the most important of these sources, and its spread was widespread in thermal applications. In practical comparison, the planet Earth receives more solar energy annually than the total energy that humans consume over an entire year. Therefore, the global effort has become focused on how to benefit from solar energy in enhancing the global economy and protecting the environment by reducing harmful emissions [2, 3].

One of the obstacles that has preoccupied researchers in this field most is how to highly benefit from incoming solar radiation because this procedure includes methods of converting solar energy into different forms of useful energy to facilitate its conservation and investment to meet the needs of human requirements. In general, the field of solar radiation investment has taken two main paths: the first is a conversion of solar energy to thermal energy by solar thermal conversion methods, and the second is a conversion of solar energy to electric energy by the solar photovoltaic method [4, 5].

One of the most important obstacles facing the implementation of the solar photovoltaic system was the issue of cooling the PV panel and reducing its temperature in the summer, especially in regions of the world characterised by hot climatic conditions. Choi et al. [6] were interested in studying the method of cooling Pv panels; the new model of water-cooling collector takes the form of a flat tunnel in contact with the bottom surface of the PV panel to absorb higher heat from the photovoltaic cells. Aluminium alloy works as a heat sink due to its high thermal conductivity.

The study included experimentally determining both electrical and thermal performance within a wide range of climatic conditions and using different mass flow ranges of water. The results focused on analysing thermal performance. The results revealed an improvement in thermal efficiency to reach a value of 40%, which was not achieved using a traditional solar heat investment device, with a significant difference of up to 0.8. The new system is characterised by a higher efficiency rate than other general systems.

Shallal et al. [7] presented an experimental and numerical analysis of the performance of the photovoltaic thermal system (PV/T) by investing nanofluids and a new collector design using sphere fins in open flow flat collector. At the same time, Ismaeel et al. [8] presented a numerical novel CFD modelling of a solar air collector integrated with a tower model for the updraft air as suggested for electrical power generation.

A solar air heater was designed with a double transparent upper skin to pass solar energy and generate the greenhouse effect, creating a hot air flow in the solar system. Ibrahim et al. [9] investigated a new design and operational environment that influences the effectiveness of hybrid solar PV/T. As a result, seven of the combinations are tailored to sorption complexes. A well-absorbed design with great efficiency was also evaluated, contrasted, and simulated (total efficiency) [10-12].

On the other hand, the mathematical models of the solar water heater (SWH) can examine various characteristics, including solar radiation, flow rate, and air temperature, and decide that the collector should be a heat collector with a flat plate and a glass plate. Through a mathematical approach, it was realised that the helical flow is the most efficient, with a maximum thermal efficiency of 50% and an electrical cell efficiency of 12% [13] in a solar roofing system. Michael and Selvarasan [14] described research on collectors for cooling PV panels by integration with a copper heat absorber. The design lowered the thermal resistance by around 9.9%, leading to an improvement in the heat transfer from solar cells to the circulating water. The Experiments were performed with various water flow rates [15, 16].

Du et al. [17] tested the radiometric features of volumetric absorbents with different porosity. The results recorded that decreasing the porosity in the inner layers of the porous media results in a more absorbent heat compared to rest types with higher porosity, and the losses in heat are lower. Experimentally, Valizade et al. [18] investigated the influence of pore size, porosity rate, and type of material on thermal characteristics. The porosity rate and pore size had a higher effect on the properties of porous media than on the type of material.

Jiandong et al. [19] used a three-dimensional numerical solution based on finite volume with steady state, and then both numerical and experimental results were compared. Three dimensions of laminar incompressible flow with steady fixed properties used continuity and energy equations with radiation models [20]. A numerical method is used to improve the effect of the metal foam substrate thickness, y, on thermal performance. The simulation results of the numerical analysis show that maximum performance takes place at 0.8 thickness for the pours layer of foam [21-23].

Solar FPCs are among the most mature and practically used solar heating technologies. Further development is required in the collector design and the selection of materials that have a high ability to absorb heat and enhance the thermal properties of the thermal fluid. The present work tested a combined enhancement of the absorbing medium and the heat carrier fluid. The included new design of a flat solar collector using aluminium porous medium (open foam) as a heat absorbing medium. Also, it increases the heat gain by enhancing the thermal properties of the working fluid by nanoadditives. Aluminum Oxide (Al_2O_3) nanoparticles have been dispersed in water to produce nanofluids. This approach is particularly increasing thermal performance in solar collectors, with fewer added costs.

2.Methods and Materials

2.1. Experimental work

A new experimental model of a flat plate SWH was designed and built to validate the prediction of the open-cell porous medium properties in improving the heat transfer process. The model was prepared for a measurement procedure. This section investigates the use of nanomaterial additives to water in an open circle. The mathematical description of flat water collector analysis used a nanofluid preparations measurement system concerning the characterisation of collector performance data collection. At the same time, the last section illustrates the uncertainty analysis.

2.1.1. Model description

The working environment influences the solar water collector's performance. The solar water collector system developed and built in this work has been put at the solar site of the University of Technology- Iraq. The data were acquired for each experimental day, starting from 07:00 am to 07:00 pm. The recorded variables in each experiment were the wind velocity, which was around 1.5±0.5 m/s, the solar radiation intensity, which was within a daily range of 21 to 998 W/m2, and the ambient air temperature, which was recorded within a range of 26 – 54 ºC.

The function of the solar water collector is to heat the working fluid during its pass through the collector by useful the solar beam falls on the outer cover of the collector. The main parameters for internal geometry in the collector included the vertical and tangential parts, and using an open cell porous medium, the temperature difference between water entering the collector and ambient air. The new design utilises an aluminium open-cell porous medium with a porosity of 80% for a high heat transfer rate and water movement in a slow, simple way; the properties of the aluminium foam are shown in Table 1.

Table 1. The properties of the aluminium foam.

Parameter	Value
Weight (average)	6.6 g
Porosity (average)	80 %
Volume (average)	2367 mm^3
Young's modulus	2366 MPa
Poisson's ratio	0.27

The collector geometry for this model comprises a block open cell porous medium with dimensions 40×60×1.5 cm and is fabricated of aluminium to allow a high heat transfer rate. This porous material was fixed uniformly in the collector body, with a 13 mm inlet and outlet diameter, as shown in Fig. 1.

2.1.2. Measuring instruments and uncertainty analysis

The solar water collector system is inclined at 30o. Thermocouples measured temperatures for different sections of the solar collector, and the water flow rate was measured by a variable area rotameter. Thermocouples Type-K were connected to a temperature reader with a selector switch and a digital thermometer. All thermocouples were calibrated. Temperature measurements are grouped into four categories. Thermocouples Group A were used for measuring the glass panel surface temperature. Thermocouples Group B were used for measuring the collector surface, and thermocouples Group C were used for measuring the inlet and outlet water temperature, as shown in Fig. 2. Details of temperature measurements, including positions, numbers, and accuracies, are shown in Table 2.

All measured parameters were included to analyse the uncertainty, solar intensity, temperatures, and water flow rates. The minimum and maximum percentage relative standard errors were determined. The maximum error values were appropriate to the experimental ranges at the same time. Table 3 shows the uncertainty values of the experimental parameters.

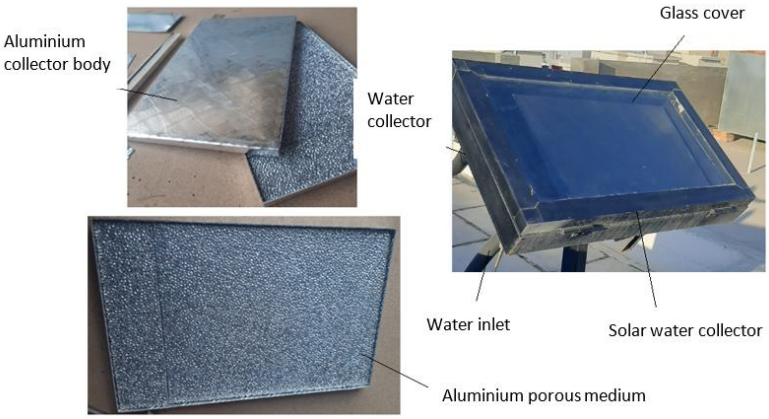

(a) The components of the FPC model.

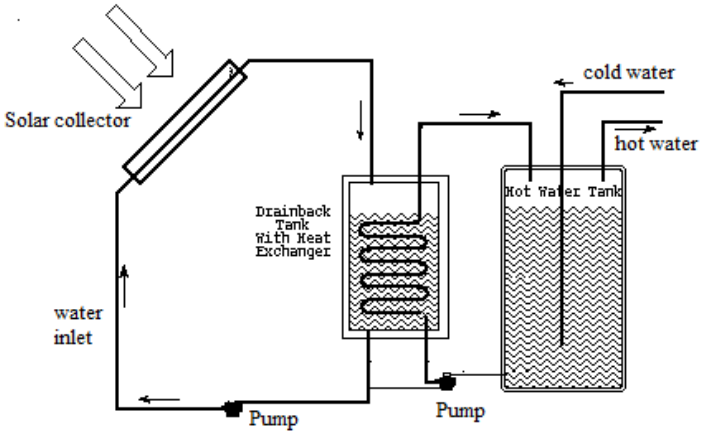

(b) Schematic diagram of the integrated SWH system.

Fig. 1. Flat plate collector and components of the solar water heating system with aluminium porous medium.

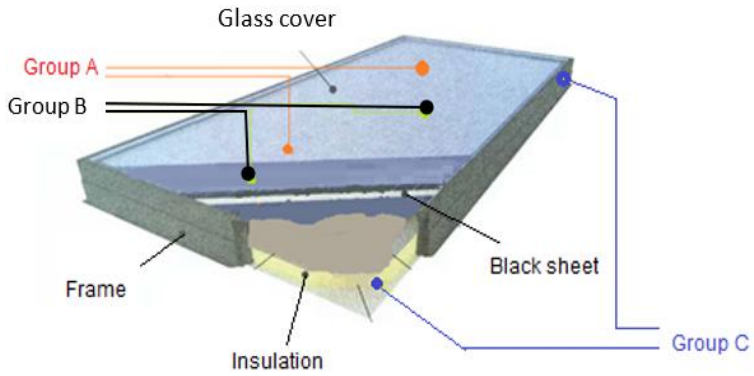

Fig. 2. Positioning schematic of temperature measurement in the collector system.

Table 2. Properties for all parts of the temperature measurement system.

No.	Type of Thermocouples	position	Accuracy	Reader Thermometer – Tm-936
1	Sensor, type-K	2 points, inlet and outlet collector	± 0.3	Accuracy ± (0.2 % + 0.5 °C)
2	Sensor, type -K	2 points on the glass cover	± 0.2	
3	Sensor, type-K	2 points on the Collector cover	± 0.2	
4	Sensor, type-K	2 points to measuring Ambient temperature, collector body	± 0.2	

Table 3. The uncertainty of the measured parameters.

Parameter	Max. value	Min. value	Min. uncertainty	Max. uncertainty
Water flow rate	3.5 l/min	1.5 l/min	±0.71	±0.52
Temperatures	78°C	23°C	±0.94	±0.65
Solar intensity	1098 W/m^2	25 W/m^2	±1.11	±1.02

2.1.3. Data acquisition

The experiments were conducted in an outdoor environment. Experimental measurements were carried out on sunny days throughout the testing period. Measurements and recording of the research variables, including water temperature, surface temperatures, wind speed, water/nanoparticles flow rate, and solar intensity, were implemented at various locations of the FPC. Also, the period time ranges were chosen from 7:00 am to 7:00 pm to provide a range for studying the performance of flat-plate solar collector heating due to solar radiation using the porous aluminium medium.

Table 4. Data collected for the modified collector system.

No.	Water flow rate (l/min)	T_{col}	$T_{w.in}$, $T_{w.out}$	T_{amb}	G (W/m^2)
Modified collector using water					
1	1.5	5 points	2 points	1 point	0-1098
2	2.5	5 points	2 points	1 point	0-1098
3	3.5	5 points	2 points	1 point	0-1098
Modified collector with Water/Al_2O_3 (2% and 3%) nanofluid					
4	1.5	5 points	2 points	1 point	0-1098
5	2.5	5 points	2 points	1 point	0-1098
6	3.5	5 points	2 points	1 point	0-1098

The experiments for the new collector with the porous medium are included. In the beginning, ambient temperature and solar intensity were measured throughout the day. The collector surface temperature and water inlet and outlet temperatures were recorded for three days for each condition with different water flow rates. Data was collected by using water/Al_2O_3 nanoparticles at different volumetric concentrations of 2% and 3%, as shown in Table 4.

2.2. Preparations of nanofluids

The preparation of nanofluid is the first main step in using nano phase particles in the heat transfer enhancement of normal fluids. To give a clear description and not allow agglomeration of nanoparticles, one must choose good ways to prepare the nanofluids, as a two-step method was selected: the first step is that the nanoparticles and distilled water are mixed directly, and the second step is the use ultrasonic vibrator for preparation of mixed aqueous nanofluid [23]. Nanofluid was prepared at concentrations of 3% by volume by adding pre-weighed quantities of nanoparticles and water. Note that the volume of pure water used in the test setup is 25 letters, and the period for mixing the nanoparticles within the preparation procedure lasted 10 minutes with continuous stirring before starting to stir them within the closed cooling cycle. The nanoparticles used in the preparation of nanofluids are Al_2O_3, with properties listed in Table 5.

Table 5. Properties for nanoparticles used.

Property	Value
Mean particles Diameter	20 nm
Heat capacity (kJ/kg·K)	765
Density (kg/m^3)	3970
Thermal conductivity (W/m·K)	40

The volume concentration of the nanoparticles in the nanofluid is evaluated by Eq. (1) [23].

$$C = \frac{volume\ of\ nanoparticle}{volume\ of\ nanoparticle + volume\ of\ water} \times 100 \quad (1)$$

$$C = \frac{(\frac{m}{\rho})_{nanoparticle}}{(\frac{m}{\rho})_{nanoparticle} + (\frac{m}{\rho})_{water}} \times 100 \quad (2)$$

2.3. Performance parameters

The collector efficiency is determined basically from three parameters: the incident solar radiation, the area of the collector, and the useful heat the collector gains [24].

$$\eta_c = \frac{Q_u}{G \times A_c} \quad (3)$$

where η_c is the efficiency of the collector, G is the incident solar radiation, A_c is the area of the collector, and Qu is the useful heat gained by the collector, it is defined as [24]:

$$\eta_c = \frac{\dot{m}_f\, Cp_f\, (T_{out} - T_{in})_f}{G \times A_c} \quad (4)$$

The heat gained by the working fluid parameters is the mass flow rate, $\dot{m}$, the heat capacity, Cp, and the change in the fluid temperature $(T_{out} - T_{in})_f$.

3. Results and Discussion

Several parameters were considered, such as the collector cover temperature, water temperature, water flow rate, solar radiation, and ambient temperature, from 07:00 am to 07:00 pm, studying the flat-plate collector system. This study was done on 16-27 May; the cloudy weather days were excluded, as were dust storms.

3.1. Effect of using porous medium and nano additives on collector temperature

Figure 3 shows the solar irradiation and ambient temperature's mean measurement results. The peak solar irradiation was recorded around midday with a value of 1140 W/m2. The ambient temperature varies between 20 to 35 °C. During the day, it is around 28 oC to 35 oC, while it drops to 20-23 oC at night.

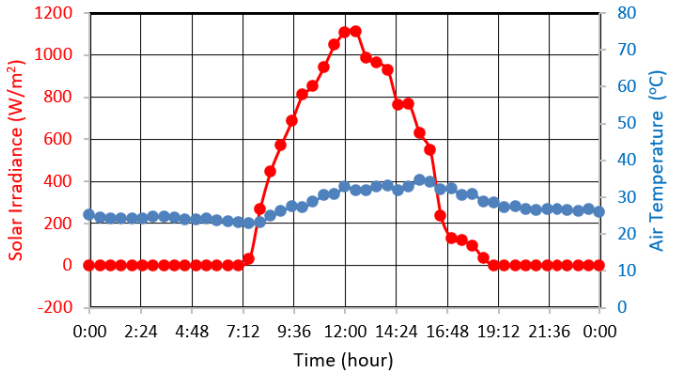

Fig. 3. Mean solar irradiation and ambient temperature values over 24 hours during the experimental measurements.

Figure 4 shows the variation of cover temperature for the collector at different conditions with and without the addition of nanoparticles. The first case includes data analysis for different water flow rates applied. Figure 4(a) shows the temperature change of the upper face of the solar collector during daylight hours. The collector cover's temperature decreases as the cooling water flow rate increases. The highest temperature was recorded for the collector cover, 52.4 oC at 12.00 pm at a water flow rate of 1.5 l/min. At the same time, the percentage of decrease was 3.1% when applying a water flow rate of 2.5 l/min, and the percentage of decrease increased to 5.6% when applying a water flow rate of 3.5 l/min.

The second case is the use of Al_2O_3 nanoparticles. Figure 4(b) shows the change of collector cover temperature during daylight hours with different volumetric concentrations of Al_2O_3 nanoparticles. The data showed a decrease in the temperature of the collector cover by 6.5% and 8% when using the Al_2O_3 nanoparticles at volumetric concentrations of 2% and 3%, respectively, at a flow rate of 3.5 l/min.

3.2. Effect of using porous medium and nano additives on water temperature

Figure 5 illustrates the variation of the temperature rise between the inlet and outlet of the coolant during daylight hours. Firstly, Fig. 5(a) shows a decrease in the difference between water temperatures ΔT with an increase in the water flow rate. It was noticed that the highest value of ΔT was 5 ℃ at a water flow rate of 1.5 l/min, while it was 2.8 and 3.7 ℃ for flow rates of 2.5 and 3.5 l/min, respectively, at the same time. Secondly, Fig. 5(b) represents the water temperature difference between the inlet and outlet of the collector, which was cooled by the addition of Al_2O_3 to water with 2 and 3% volumetric concentrations recorded during daylight hours at a flow rate of 3.5l/min. It clearly noticed an increase ΔT when using Al_2O_3

nanofluid as a coolant with a volumetric concentration of 2% by 45% than using water only, while ΔT increased by 48% when a coolant with a volumetric concentration was 3%.

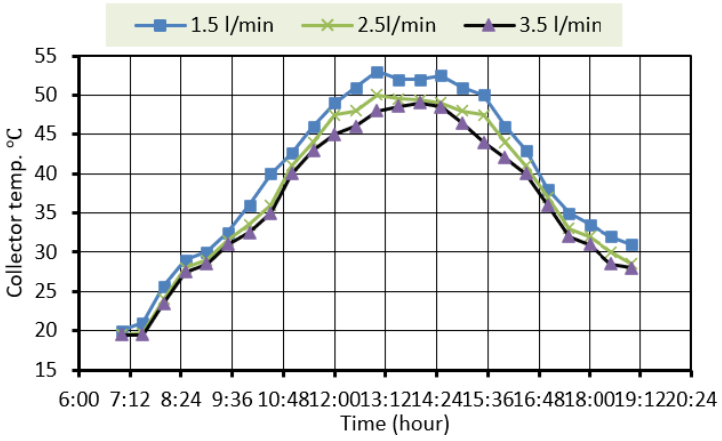

(a) Different water flow rates.

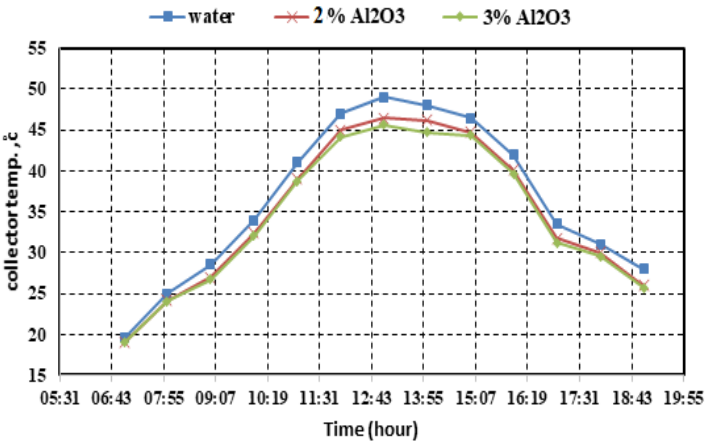

(b) Different concentrations of Al_2O_3 Nanofluid.

Fig. 4. Variation of collector temperature during the day.

The effect of nanomaterials, according to the mechanism of their kinetic diffusion and fluctuation within the cooling fluid, makes the flow behaviour of the fluid more like a turbulent state with a tangential temperature gradient in the greatest content of the fluid, which leads to improved heat transfer by convection of nanofluids. On the other hand, at high flow ranges (higher Reynolds numbers), this vision changes and becomes no longer dominant. I.e., heat transfer does not depend more on the fluid's conductivity, and the thermal conductivity effect is less obvious. While in the presence of nanomaterials, the rate of improvement in heat transfer mentioned above decreases with increasing flow rate.

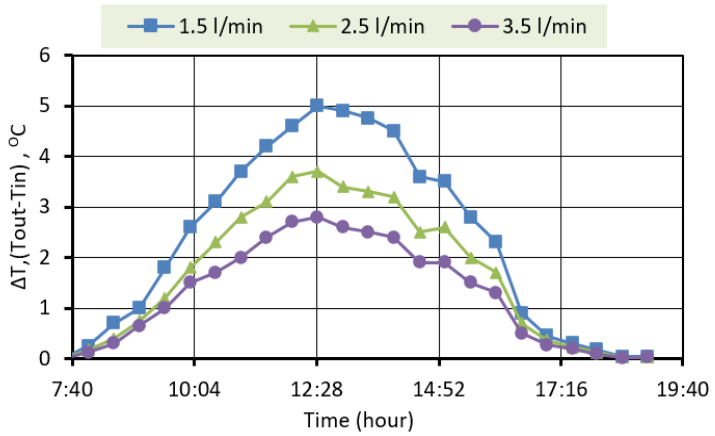

(a) Different water flow rates.

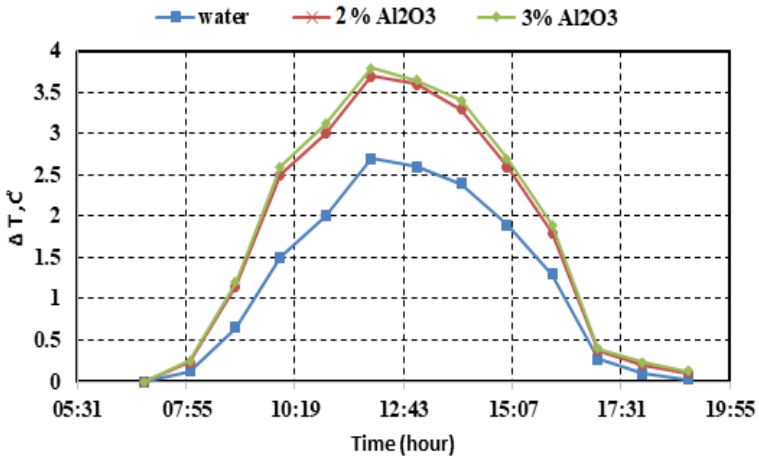

(b) Different concentrations of Al_2O_3 nanofluid at flow rate 3.5 l/min.

Fig. 5. Variation of the temperature difference between the inlet and outlet of the coolant during the day

3.3. Effect of using porous medium and nano additives on collector thermal efficiency

Figure 6 shows the results of the collector's thermal efficiency calculated for different cases. Figure 6(a) shows the collector efficiency at changing flow rates of 1.5, 2.5, and 3.5 l/min. It recorded an increase in collector efficiency at high flow rates. The data was compared for the applied flow rates at 12:00 pm. The thermal efficiency results were recorded as 13.5% and 18.4% when using the flow rates of 2.5 and 3.5 l/min, respectively. Figure 6(b) describes the collector's thermal efficiency during daylight hours for different concentrations of Al_2O_3 nanofluids. Thermal efficiency was increased with an increase in the concentration of 2% Al_2O_3 and 3% Al_2O_3 at the same flow rate of 3.5 l/min. Results show that using

Al_2O_3/water at a volumetric concentration of 2% and 3% increases the thermal efficiency by 27.6% and 38.4 %, respectively.

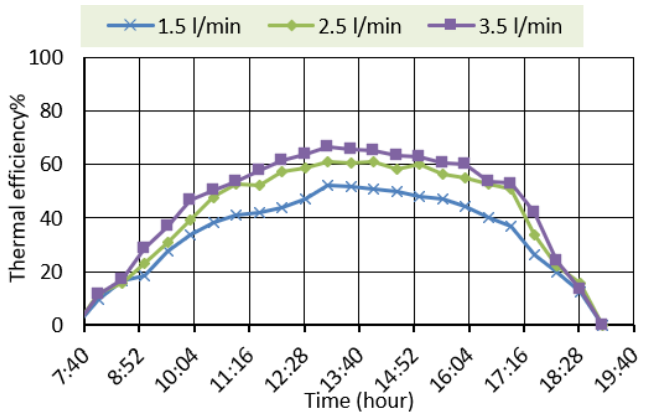

(a) Different water flow rates.

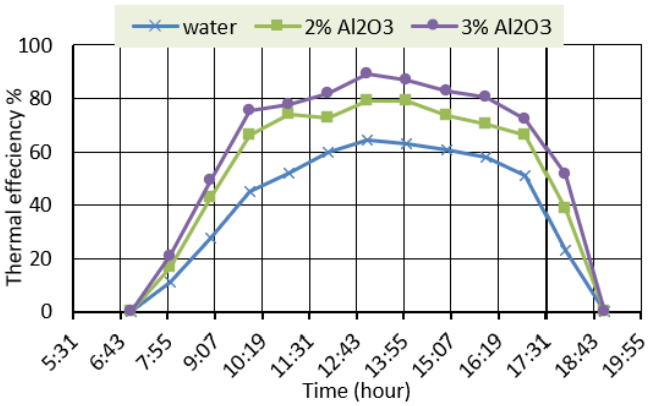

(b) Different concentrations of Al_2O_3 nanofluid at a flow rate of 3.5 l/min.

Fig. 6. Variation of the collector thermal efficiency.

The amount of heat energy obtained using the hybrid porous medium with the added nanomaterials inside the collector is proportional to the thermal energy in the collection area and solar radiation, which led to improving the collector's efficiency. This efficiency enhancement is attributed to the improvement in heat transfer resulting from the addition of nanomaterials. The initial temperature rise of the storage fluid contributed to preserving heat loss, thus increasing the system's efficiency. On the other hand, increasing the higher nanomaterial concentration contributed to increasing the efficiency due to the decrease in thermal conductivity resulting from the aggregation of nanoparticles.

Previous work using integrated Aluminum foam is reported by Owolabi Afolabi et al. [25]. They also embedded the Aluminum foam underneath the absorbing plate in flat plate SWH. They claimed that their experiment demonstrated that the

efficiency of the flat plate SWH system has been enhanced from 47.5% when operating without TES to 52.2% when operating with PCM-TES with AL foam cells underneath the absorber. Furthermore, it was further enhanced to 57.5% when nanocomposite-TES was used. This trend of similarity in the enhancement confirms the effectiveness of Al foam usage in the SWH systems.

4. Conclusions

This work presents an experimental analysis of the flat-plate solar collector performance using nano additives with a new collector design using a porous medium as an absorbing and heat transfer medium. The following conclusions have been drawn from the results achieved.

- The collector cover temperature decreased with increasing flow rate when water was used as the cooling fluid. It noted that using 2% Al_2O_3 reduces the temperature of the collector cover at 6.5% and decreases by 8% when using Al_2O_3 by a volumetric concentration of 3% for a flow rate of 3.5 l/min.
- The results recorded an increase in collector thermal efficiency with an increase in the flow rate. It increased by 13.5% and 18.4% when flow rates increased from 1.5 l/min to 2.5 and 3.5 l/min, respectively.
- Using Al_2O_3/water at a volumetric concentration of 2% and 3% increases the thermal efficiency by 27.6% and 38.4 %, compared to water as a thermal fluid, respectively.

The experimental results performed in this study revealed that using an open cell porous cell medium and adding nanoparticles to the coolant fluid show commendable performance in converting solar radiation into thermal energy.

Nomenclatures

A_c	Area of collector, m^2
C	Volume concentration, %
Cp	Heat Capacity, kJ/kg·K
F_r	The proportion of actual useful energy gain.
G	Solar irradiation incident on the glass cover, W/m^2
$\dot{m}$	Mass flowrate, kg/s
Q_u	Useful heat gain, W
T_a	Atmospheric Temperature, K or ^oC
T_i	Temperature of fluid entering collector, K or ^oC
T_o	Temperature of fluid exits the collector, K or ^oC
T_p	The average temperature of the absorber plate, K or ^oC
V_f	Volume flow rate, l/min

Greek Symbols

η_c	Collector efficiency, %
ρ	Density, kg/m^3

Abbreviations

Al_2O_3	Aluminium oxide
SWH	Solar Water Heater

References

1. IRENA (2022), Renewable Energy Statistics 2022, *International Renewable Energy Agency*, Abu Dhabi.
2. Wahhab, H.A.A.; and Al-Maliki, W.A.K. (2020). Application of a solar chimney power plant to electrical generation in covered agricultural fields. *Proceedings of the 3rd International Conference on Engineering Sciences*, *IOP Conference Series*: *Materials Science and Engineering*, Kerbala, Iraq.
3. Assaf, Y.H.; Akroot, A.; Abdul Wahhab, H.A.; Talal, W.; Bdaiwi, M. and Nawaf, M.Y. (2023). Impact of nano additives in heat exchangers with twisted tapes and rings to increase efficiency: A review. *Sustainability*, 15, 7867.
4. Chopra, K.; Pathak, A.K.; Tyagi, V.V.; Pandey, A.K.; Anand, S. and Sari, A. (2020). Thermal performance of phase change material integrated heat pipe evacuated tube solar collector system: An experimental assessment. *Energy Conversion and Management*, 203, 112205.
5. Dubey, S.; and Tay, A.A. (2013). Testing of two different types of photovoltaic–thermal (PVT) modules with heat flow pattern under tropical climatic conditions. *Energy for Sustainable Development*, 17(1), 1-12.
6. Choi, H.U.; and Choi, K.H. (2020). Performance evaluation of PV/T air collector having a single-pass double-flow air channel and non-uniform cross-section transverse rib. *Energies*, 13(9), 2203.
7. Shallal, B.A.; Gedik, E.; Wahhab, H.A.A. and Ajel, M.G. (2023). Impact of alumina nanoparticles additives on open-flow flat collector performance for PV panel thermal control application. *Evergreen*, 10(2).
8. Ismaeel, A.A.; Abdul Wahhab, H.A.; and Naji, Z.H. (2021). Performance evaluation of updraft air tower power plant integrated with double skin solar air heater. *Evergreen*, 8, 296-303.
9. Ibrahim, A.; Othman, M.Y.; Ruslan, M.H.; Alghoul, M.; Yahya, M.; Zaharim, A.; and Sopian, K. (2009). Performance of photovoltaic thermal collector (PVT) with different absorbers design. *WSEAS Transactions on Environment and Development*, 5(3), 321-330.
10. Kishore, R.A.; Bianchi, M.V.; Booten, C.; Vidal, J.; and Jackson, R. (2021). Enhancing building energy performance by effectively using phase change material and dynamic insulation in walls. *Applied Energy*, 283, 116306.
11. Nawaf, M.Y.; Akroot, A. and Wahhab, H.A.A. (2023). Numerical simulation of a porous media solar collector integrated with thermal energy storage system. *Journal of Engineering Science and Technology*, *Special Issue on Development of Sustainability Systems - I*, 117 – 130.
12. Sadeghi, G.; Najafzadeh, M.; Ameri, M.; and Jowzi, M. (2022). A case study on copper-oxide nanofluid in a back pipe vacuum tube solar collector accompanied by data mining techniques. *Case Studies in Thermal Engineering*, 32, 101842.
13. Rahou, M.; Othman, M.Y.; Mat, S. and Ibrahim, A. (2014). Performance study of a photovoltaic thermal system with an oscillatory flow design. *Journal of Solar Energy Engineering*, 136(1), 011012.

14. Michael, J.J.; and Selvarasan, I. (2017). Experimental investigation of a copper sheet-laminated solar photovoltaic thermal water collector. *Energy Efficiency*, 10(1), 117-128.
15. Gorjian, S.; Ebadi, H.; Najafi, G.; Chandel, S.S.; and Yildizhan, H. (2021). Recent advances in net zero energy greenhouses and adapted thermal energy storage systems. *Sustainable Energy Technologies and Assessments*, 43, 100940.
16. Al-Shamani, A.N.; Sopian, K.; Mat, S.; Hasan, H.A.; Abed, A.M.; and Ruslan, M.H. (2016). Experimental studies of rectangular tube absorber photovoltaic thermal collector with various types of nano fluids under the tropical climate conditions. *Energy Conversion and Management*, 124, 528-542.
17. Du, S.; Ren, Q.; and He, Y.L. (2017). Optical and radiative properties analysis and optimisation study of the gradually varied volumetric solar receiver. *Applied Energy*, 207, 27-35.
18. Valizade, M.; Heyhat, M.M.; and Maerefat, M. (2019). Experimental comparison of optical properties of nanofluid and metal foam for using in direct absorption solar collectors. *Solar Energy Materials and Solar Cells*, 195, 71-80.
19. Jiandong, Z.; Hanzhong, T.; Susu, C. (2015). Numerical simulation for structural parameters of flat-plate solar collector. *Solar Energy*, 117, 192-202.
20. Podder, B.; and Biswas, A. (2019). Experimental analysis of the performance of a solar photovoltaic-thermal (pv/t) water collector with a modified absorber design for the climatic condition of Assam. *NISCAIR-CSIR*, India, 437-441.
21. Ekramian, E.E.S.H.M.; Etemad, S.G. and Haghshenasfard, M. (2014). Numerical analysis of heat transfer performance of flat plate solar collectors. *Journal of Fluid Flow Heat and Mass Transfer*, 1, 38-42.
22. Saedodin, S.; Zamzamian, S.A.H.; Eshagh Nimvari, M.S.; Wongwises, H.; Jouybari, J. (2017). Performance evaluation of a flat-plate solar collector filled with porous metal foam: Experimental and numerical analysis Author links open overlay panel. *Energy Conversion and Management*, 153, 278-287.
23. Shamshirgaran, S.R.; Al-Kayiem, H.H.; Sharma, K.V.; and Ghasemi, M. (2020). State of the art of techno-economics of nanofluid-laden flat-plate solar collectors for sustainable accomplishment. *Sustainability*, 12(21), 9119.
24. Al-Kayiem, H.H.; and Lin, S.C. (2014). Performance evaluation of a solar water heater integrated with a PCM nanocomposite TES at various inclinations. *Solar Energy*, 109, 82-92.
25. Owolabi Afolabi, L.; H Al-Kayiem, H. and B Aklilu, T. (2017). On the nano-additive enhanced flat plate solar collector integrated with thermal energy storage. *Nanoscience and Nanotechnology-Asia*, 7(2), 172-182.